

# Expressions of dissipated powers and stored energies in poroelastic media modeled by $\{\mathbf{u}, \mathbf{U}\}$ and $\{\mathbf{u}, P\}$ formulations

Olivier Dazel<sup>a)</sup>

Laboratoire d'Acoustique de l'Université du Maine — UMR CNRS 6613, Avenue Olivier Messiaen,  
F-72 085 Le Mans Cedex, France

Franck Sgard and François-Xavier Becot

Département Génie Civil et Bâtiment-URA CNRS 1652, Ecole Nationale des Travaux Publics de l'Etat,  
F-69518 Vaulx-en-Velin Cedex, France

Noureddine Atalla

Groupe Acoustique de l'Université de Sherbrooke, 2500 Boulevard de l'Université, Sherbrooke,  
Quebec J1K2R1, Canada

(Received 3 October 2006; revised 10 January 2008; accepted 18 January 2008)

This paper is devoted to the rigorous obtention of the energy balance in porous materials. The wave propagation in the porous media is described by Biot-Allard's  $\{\mathbf{u}, \mathbf{U}\}$  and  $\{\mathbf{u}, P\}$  formulations. The paper derives the expressions for stored kinetic and strain energies together with dissipated energies. It is shown that, in the case of mixed formulations, these expressions do not correspond to the real and imaginary parts of the variational formulations. A quantitative convergence analysis of finite element scheme is then undertaken with the help of these indicators. It is shown that the order of convergence of these indicators for linear finite-element is one and that they are then well fitted to check the validity of finite-element models.

© 2008 Acoustical Society of America. [DOI: 10.1121/1.2874520]

PACS number(s): 43.55.Ev, 43.20.Bi [KA]

Pages: 2054–2063

## I. INTRODUCTION

Porous materials are commonly used in noise control issues as passive devices for reducing both structure and airborne sound. Today, most of the vibroacoustic prediction tools are able to account for the coupling of structures with a porous medium. These tools are mainly based on Biot-Allard's<sup>1,2</sup> model. In noise control analysis, it is often desirable to understand how energy is stored and how power flows from one system component to the other. Two sets of poroelastic formulations can be distinguished: The first one deals with displacement formulations<sup>1,2</sup> and the second one is concerned with mixed formulations.<sup>3–5</sup> The finite-element modeling of porous material by the way of  $\{\mathbf{u}, \mathbf{U}\}$ <sup>6,7</sup> techniques or  $\{\mathbf{u}, P\}$ <sup>4,5</sup> techniques.  $\{\mathbf{u}, P\}$  finite-element methods have shown their efficiency compared to displacement formulation<sup>4,5</sup> and a key point to improve them is to study their convergence and their physical interpretation. Due to the biphasic nature of porous materials and also to the fact that in mixed pressure-displacement formulations the fields are of different nature, the derivation of the expressions of energies and powers in these media is not obvious; in particular they cannot be obtained through separating the real and imaginary parts of the variational formulations. In the past, only equations related to the dissipated powers have been presented in the case of Biot-Allard's  $\{\mathbf{u}, P\}$  formulations.<sup>8–10</sup> The first objective of this paper is to rigorously derive the expressions of both stored and dissipated

energies in poroelastic materials based on the theorem of kinetic energy in the framework of  $\{\mathbf{u}, \mathbf{U}\}$  and  $\{\mathbf{u}, P\}$  formulations of Biot-Allard's poroelasticity equations. The second objective of this paper is to propose a quantitative convergence analysis of finite element scheme with the help of these indicators. This analysis shows that these indicators are of order one and can advantageously be used to check the validity of finite-element schemes.

In the following, the considered porous medium are usual sound absorbing materials like fibrous aggregates and foams. As acoustical applications are considered, the porous skeleton is assumed to be fully saturated by air. According to Biot's theory, the porous medium is considered as a superposition of a solid phase and fluid phase described by homogenized fields.  $K$  (respectively,  $W$ ) denotes the total kinetic (respectively, strain) energy of the porous media. The separation of these two quantities into a solid part and a fluid part must be handled with particular care since one deals with homogenized quantities. In the porous material, three dissipation mechanisms associated with viscous and thermal effects together with structural damping occur. Unlike stored energies, the derivation of the dissipated powers into a solid and fluid part is more tractable since the physical phenomenon is intrinsically linked to a particular phase (solid phase for structural damping and fluid phase for viscous and thermal effects).

In this paper, a temporal dependency  $e^{j\omega t}$  is chosen. For a given quantity  $X$ , an index 0 will represent its complex amplitude so that  $X = X_0 e^{j\omega t}$ .  $\mathcal{R}(\cdot)$  and  $\mathcal{I}(\cdot)$  denote the real part and imaginary part functions of complex numbers, the star exponent is associated with the complex conjugation.

<sup>a)</sup>Electronic mail: olivier.dazel@univ-lemans.fr

Moreover, for all inertial and constitutive coefficients appearing in the model, a  $(\sim)$  above a coefficient indicates that it is complex-valued and frequency-dependent.  $Y_r$  and  $Y_i$  refer to the real part and imaginary part of  $\tilde{Y}$ , respectively.

The classical techniques, dealing with the real and imaginary parts of variational formulations, must be handled with care in the case of poroelastic problems. Hence, the methodology of our derivation is to express in the time domain the kinetic energy theorem and the thermodynamics first principle. Both of these theorems are expressed in the case of the  $\{\mathbf{u}, \mathbf{U}\}$  formulation as this one is fitted for a clear explanation and separation of the different physical mechanisms. This first step is, by itself, not original and has been applied in previous works for geomaterials.<sup>1,11</sup> Nevertheless, it has never been applied to acoustical materials involving frequency-dependent parameters and the link with the poroelastic  $\{\mathbf{u}, \mathbf{U}\}$  variational formulations has never been established. This first step is also interesting as the different notations and mechanisms can be defined. Once the temporal expressions of stored energies and dissipated powers are written, their mean value over a vibrating cycle can easily be obtained. The expressions of these indicators in the case of the  $\{\mathbf{u}, P\}$  formulation are directly derived from the one of the displacement formulation through a variable change. Hence, no energetic demonstration is done in the case of the mixed formulation, but the expressions are derived from the displacement ones.

This paper is organized as follows. First, the equations of motion and stress–strain relationships for a saturated poroelastic material are recalled (Sec. II). Then the expressions of stored and dissipated energies are derived in the case of  $\{\mathbf{u}, \mathbf{U}\}$  formulation (Sec. III). These expressions are then provided in the case of the  $\{\mathbf{u}, P\}$  formulation (Sec. IV). A simple example is then presented in order to illustrate and a quantitative and original convergence investigation of a finite-element scheme, based on the proposed indicators, is finally described in Sec. V.

## II. OVERVIEW OF BIOT'S EQUATIONS

For sake of clarity, Biot–Allard's poroelasticity equations are first recalled in order to identify the different terms appearing in the expressions of the energies given in the following.

### A. Equations of motion

The equations of motion of  $\{\mathbf{u}, \mathbf{U}\}$  formulation are<sup>1</sup>

$$-\omega^2 \rho_1 \mathbf{u} = \nabla \cdot \boldsymbol{\sigma}^s(\mathbf{u}, \mathbf{U}) + \omega^2 \rho_{12}(\mathbf{U} - \mathbf{u}) + j\omega \tilde{b}(\mathbf{u} - \mathbf{U}), \quad (1a)$$

$$-\omega^2 \rho_2 \mathbf{U} = \nabla \cdot \boldsymbol{\sigma}^f(\mathbf{u}, \mathbf{U}) + \omega^2 \rho_{12}(\mathbf{u} - \mathbf{U}) - j\omega \tilde{b}(\mathbf{u} - \mathbf{U}). \quad (1b)$$

$\boldsymbol{\sigma}^s(\mathbf{u}, \mathbf{U})$  [respectively,  $\boldsymbol{\sigma}^f(\mathbf{u}, \mathbf{U})$ ] denotes the partial stress tensor of the solid (respectively, fluid) phase.  $\rho_1$ ,  $\rho_2$ , and  $\rho_{12}$  represent homogenized densities. They are given by

$$\rho_1 = (1 - \phi)\rho_s, \quad \rho_2 = \phi\rho_f, \quad \rho_{12} = -\phi\rho_f(\alpha_\infty - 1). \quad (2)$$

$\phi$  is the porosity,  $\rho_s$  is the skeleton material density,  $\rho_f$  is the interstitial fluid density, and  $\alpha_\infty$  refers to geometric tortuosity.  $\rho_{12}$  accounts for the interaction between the inertia forces of the solid and fluid phase.  $(j\omega)\tilde{b}(\mathbf{u} - \mathbf{U})$  represents the contribution of viscous forces. It is worth noting that the real part  $b_r$  and imaginary part  $b_i$  of  $\tilde{b}$  are respectively associated with the dissipative part of viscous forces and with the modification of tortuosity due to the added mass effect associated with the viscous behavior of the fluid in the pores. In order to simplify Eqs. (1a) and (1b) an apparent inertial mass can be introduced,

$$\tilde{\rho}_{12} = \rho_{12} - \frac{\tilde{b}}{j\omega} = \underbrace{\left(\rho_{12} - \frac{b_i}{\omega}\right)}_{\rho'_{12}} + j\frac{b_r}{\omega},$$

hence the last two terms on the right-hand side of Eq. (1) can be grouped; this new coefficient provides a more compact writing but hides the two different phenomena (geometry and viscosity) in the real part (denoted by  $\rho'_{12}$ ).

### B. Constitutive relations

In order to identify all the macroscopical coefficients, stress–strain relations must be considered. They read:<sup>1,12</sup>

$$\boldsymbol{\sigma}^s(\mathbf{u}, \mathbf{U}) = \tilde{A} \nabla \cdot \mathbf{u}\mathbf{I} + 2\hat{N}\boldsymbol{\varepsilon}^s(\mathbf{u}) + \tilde{Q} \nabla \cdot \mathbf{U}\mathbf{I}, \quad (3a)$$

$$\boldsymbol{\sigma}^f(\mathbf{u}, \mathbf{U}) = \tilde{R} \nabla \cdot \mathbf{U}\mathbf{I} + \tilde{Q} \nabla \cdot \mathbf{u}\mathbf{I}. \quad (3b)$$

$\boldsymbol{\varepsilon}^s(\mathbf{u})$  is the strain tensor of the fluid phase and  $\mathbf{I}$  is the identity tensor of rank 3. All the constitutive coefficients but  $\hat{N}$  are also complex and frequency dependent and their expression can be found in Biot and Willis's work.<sup>12</sup> Their complex and frequency-dependent nature is due to thermal effects; the real part corresponds to conservative effects (stress) and the imaginary part to thermal dissipative effects. It is important to note that  $\tilde{A}$  is frequency dependent but can be split into two terms as

$$\tilde{A} = \hat{A} + \frac{\tilde{Q}^2}{\tilde{R}}, \quad (4)$$

where  $\hat{A}$  is linked to the property of the solid *in vacuo* and  $\tilde{Q}^2/\tilde{R}$  can be related to a restoring elastic force induced by the fluid phase on the solid phase. One can then introduce the *in vacuo* solid stress tensor:

$$\hat{\boldsymbol{\sigma}}(\mathbf{u}) = \hat{A} \nabla \cdot \mathbf{u}\mathbf{I} + 2\hat{N}\boldsymbol{\varepsilon}(\mathbf{u}). \quad (5)$$

Unlike the partial stress tensor of the solid part,  $\hat{\boldsymbol{\sigma}}(\mathbf{u})$  is independent of the motion of the fluid phase; in addition its constitutive coefficients do not depend on frequency since the contribution of the fluid phase has been withdrawn. This tensor plays an important role in the mixed formulation. Another interesting property is that in all cases, the ratio  $\tilde{Q}/\tilde{R}$  is real so that a useful nondimensional real parameter can be defined

$$\xi = \frac{\tilde{Q}}{\tilde{R}} = \frac{Q_r}{R_r} = \frac{Q_i}{R_i} \in \mathbb{R}. \quad (6)$$

In order to take into account dissipation in the porous skeleton a hysteretic model is often used and it is then assumed that

$$\hat{A} = A_r + jA_i = A(1 + j\eta_s), \quad \hat{N} = N_r + jN_i = N(1 + j\eta_s), \quad (7)$$

where  $\eta_s$  is the skeleton structural damping coefficient. Note that other damping models can be substituted. In order to make a distinction between conservative and dissipative effects let  $\hat{\sigma}_r^s(\mathbf{u})$  [respectively,  $\hat{\sigma}_i^s(\mathbf{u})$ ] be the *in vacuo* tensor associated to the real (respectively, imaginary) part of coefficients.

### III. EXPRESSIONS OF ENERGIES AND POWERS IN THE CASE OF $\{\mathbf{u}, \mathbf{U}\}$ FORMALISM

#### A. Theorem of kinetic energy

The theorem of kinetic energy should be first expressed for Biot's equations. The methodology is inspired from the one presented in Ref. 11 and is based on the mechanics and thermodynamics of open continuous media. This paper extends Coussy's purpose to the case of acoustic materials and gives explicit expressions of all the terms of both  $\{\mathbf{u}, \mathbf{U}\}$  and  $\{\mathbf{u}, P\}$  formulations which are not given in detail in the previous references.

The theorem of kinetic energy is a particular case of the theorem of virtual powers. This theorem stipulates that for any material subdomain and for any velocity field whether actual or virtual, the sum of the powers of external, inertia, and internal forces is zero; the kinetic energy corresponds to the case of the actual velocity field. In order to obtain the expression of theorem of virtual powers, the temporal point of view must be considered; hence, by introducing  $\mathbf{v}$  (respectively,  $\mathbf{V}$ ), the complex velocity field of the solid (respectively, fluid) phase, Eq. (1) is rewritten in the time domain as

$$\begin{aligned} \rho_1 \frac{d\mathcal{R}(\mathbf{v})}{dt} + \rho'_{12} \frac{d}{dt} \mathcal{R}(\mathbf{V} - \mathbf{v}) \\ = \mathcal{R}(\nabla \cdot \boldsymbol{\sigma}^s(\mathbf{u}, \mathbf{U})) - b_r \mathcal{R}(\mathbf{v} - \mathbf{V}), \end{aligned} \quad (8a)$$

and

$$\begin{aligned} \rho_2 \frac{d\mathcal{R}(\mathbf{V})}{dt} + \rho'_{12} \frac{d}{dt} \mathcal{R}(\mathbf{v} - \mathbf{V}) \\ = \mathcal{R}(\nabla \cdot \boldsymbol{\sigma}^f(\mathbf{u}, \mathbf{U})) - b_r \mathcal{R}(\mathbf{V} - \mathbf{v}). \end{aligned} \quad (8b)$$

In order to obtain the kinetic energy theorem, Eq. (8a) [respectively, (8b)] is multiplied by  $\mathcal{R}(\mathbf{v})$  [respectively,  $\mathcal{R}(\mathbf{V})$ ], both equations are integrated on the porous domain  $\Omega$  and the sum of the two obtained equations is performed. The resulting term corresponding to the left-hand side of Eqs. (8a) and (8b) can be interpreted as the total derivative of the total kinetic energy  $K$  defined by

$$K = \frac{1}{2} \int_{\Omega} \rho_1 \mathcal{R}^2(\mathbf{v}) + \rho_2 \mathcal{R}^2(\mathbf{V}) - \rho'_{12} \mathcal{R}^2(\mathbf{V} - \mathbf{v}) d\Omega. \quad (9)$$

In order to distinguish the powers of external and internal forces, Green's second formula is used and the term corresponding to the right-hand side of Eqs. (8a) and (8b) then reads:

$$\begin{aligned} P_{\text{ext}} = \oint_{\partial\Omega} \mathcal{R}(\boldsymbol{\sigma}^s(\mathbf{u}, \mathbf{U})) \cdot \mathcal{R}(\mathbf{v}) \cdot \mathbf{n} d\Gamma \\ + \oint_{\partial\Omega} \mathcal{R}(\boldsymbol{\sigma}^f(\mathbf{u}, \mathbf{U})) \cdot \mathcal{R}(\mathbf{V}) \cdot \mathbf{n} d\Gamma, \end{aligned} \quad (10)$$

$$\begin{aligned} P_{\text{int}} = \int_{\Omega} \mathcal{R}(\boldsymbol{\sigma}^s(\mathbf{u}, \mathbf{U})) : \mathcal{R}(\mathbf{d}^s) + \mathcal{R}(\boldsymbol{\sigma}^f(\mathbf{u}, \mathbf{U})) : \mathcal{R}(\mathbf{d}^f) \\ - b_r \mathcal{R}(\mathbf{v} - \mathbf{V})^2 d\Omega, \end{aligned} \quad (11)$$

where  $\mathbf{d}^s$  and  $\mathbf{d}^f$  are the time derivatives of strain tensors associated with the solid phase and fluid phase, respectively. The kinetic energy theorem is then in its classical form:

$$\mathcal{P}_{\text{ext}} = \mathcal{P}_{\text{int}} + \frac{DK}{Dt}. \quad (12)$$

#### B. Expression of the first law

For dissipative media, the only use of the kinetic energy theorem is not sufficient to detail and separate the different aspects of energy stored and exchanged by the porous media. It is necessary to use the first law of thermodynamics, which expresses the conservation of energy in all its forms. This principle states that at any time, the material derivative of the total energy  $\mathcal{E}$  is equal to the sum of the work rate  $\mathcal{P}_{\text{ext}}$  of the external forces acting upon the porous material and of the rate  $\mathcal{Q}^0$  of external heat supply. The total energy is in fact the sum of the kinetic energy  $K$  defined in the following and of the internal energy  $E$  associated with both the deformation of the media and the random, disordered motion of molecules at atomic scale:

$$\frac{D\mathcal{E}}{Dt} = \mathcal{P}_{\text{ext}} + \mathcal{Q}^0. \quad (13)$$

In the classical models used in acoustics of porous media, it is always assumed that this internal energy is only due to deformation effects without modification of the temperature of the matter. This is due to the high ratio of thermal conductivity to thermal capacity in both media which causes all the heat produced by dissipation mechanisms to go outside of the porous medium without warming it up.

By combining Eqs. (12) and (13), one obtains

$$\frac{DE}{Dt} = \mathcal{Q}^0 + \mathcal{P}_{\text{int}}. \quad (14)$$

Hence, the integration over a cycle of equations (12) and (13) leads to

$$\int_T \mathcal{P}_{\text{ext}} dt = \int_T \mathcal{P}_{\text{int}} dt = - \int_T \mathcal{Q}^0 dt. \quad (15)$$

The interpretation is as follows: If over a cycle, mechanical energy is algebraically provided to the system, an equal amount of heat is released by the porous medium; in other words, no energy is stored in the porous media. The transformation of nature of energy is due to the dissipation phenomena inside the porous medium which is more easily understandable by detailing  $\mathcal{P}_{\text{int}}$ . The latter is the sum of four terms:

$$\mathcal{P}_{\text{int}} = dW_{\text{def}} - \mathcal{P}_{\text{vis}} - \mathcal{P}_{\text{str}} - \mathcal{P}_{\text{th}} \quad (16)$$

$dW_{\text{def}}$  corresponds to the conservative elastic effects defined by

$$dW_{\text{def}} = \int_{\Omega} \hat{\sigma}_r^s(\mathcal{R}(\mathbf{u})) : \mathcal{R}(\mathbf{d}^s) + R_r \nabla \cdot \mathcal{R}(\xi \mathbf{u} + \mathbf{U}) \nabla \cdot \mathcal{R}(\xi \mathbf{v} + \mathbf{V}) d\Omega. \quad (17)$$

$dW_{\text{def}}$  is the material derivative of the strain energy  $W_{\text{def}}$  defined by

$$W_{\text{def}} = \frac{1}{2} \int_{\Omega} \hat{\sigma}_r^s(\mathcal{R}(\mathbf{u})) : \mathcal{R}(\boldsymbol{\varepsilon}^s) + R_r (\nabla \cdot \mathcal{R}(\xi \mathbf{u} + \mathbf{U}))^2 d\Omega. \quad (18)$$

$P_{\text{vis}}$ ,  $P_{\text{str}}$ ,  $P_{\text{th}}$  are the powers dissipated by viscous effects, structural damping, and thermal effects. They read:

$$P_{\text{vis}} = \int_{\Omega} b_r \mathcal{R}^2(\mathbf{v} - \mathbf{V}) d\Omega, \quad (19a)$$

$$P_{\text{str}} = \int_{\Omega} \hat{\sigma}_i^s(\mathcal{I}(\mathbf{u})) : \mathcal{R}(\mathbf{d}^s) d\Omega, \quad (19b)$$

$$P_{\text{th}} = \int_{\Omega} R_i \nabla \cdot \mathcal{I}(\xi \mathbf{u} + \mathbf{U}) \nabla \cdot \mathcal{R}(\xi \mathbf{v} + \mathbf{V}) d\Omega. \quad (19c)$$

### C. Separation of energies stored in the solid and fluid part

The distinction between the solid and fluid is now undertaken to separate the contribution of each phase to  $K$  and  $W_{\text{def}}$ .

The definition (9) of the kinetic energy  $K$  comprises three terms. The first one can be interpreted as the kinetic energy of the solid phase  $K_s$ :

$$K_s = \frac{1}{2} \int_{\Omega} \rho_1 \mathcal{R}^2(\mathbf{v}) d\Omega. \quad (20)$$

The last two terms represent the kinetic energy of the fluid phase  $K_f$ :

$$K_f = \frac{1}{2} \int_{\Omega} \rho_2 \mathcal{R}^2(\mathbf{V}) - \rho'_{12} \mathcal{R}^2(\mathbf{V} - \mathbf{v}) d\Omega. \quad (21)$$

Let us now consider the strain energy. In Eq. (18), two terms appear. The first term (referred to in the following as  $\hat{W}_{\text{def}}^s$ ) can easily be defined as the strain energy of the *in vacuo* solid phase. To interpret the second part, the stress-strain relation of the fluid phase must be considered. Since

$$- \phi \frac{P}{\tilde{R}} = \xi \nabla \cdot \mathbf{u} + \nabla \cdot \mathbf{U}, \quad (22)$$

the second term can be expressed and defined as

$$\hat{W}_{\text{def}}^f = \frac{1}{2} \phi^2 R_r \int_{\Omega} \mathcal{R}^2 \left( \frac{P}{\tilde{R}} \right) d\Omega, \quad (23)$$

which can be interpreted as the strain energy of a closed fluid media. Nevertheless neither the solid is *in vacuo*, nor the media is closed. The best way to separate the solid and fluid phase is to go back to the partial stress tensor. Hence:

$$\begin{aligned} W_{\text{def}}^s &= \frac{1}{2} \int_{\Omega} \mathcal{R}(\boldsymbol{\sigma}^s(\mathbf{u}, \mathbf{U})) : \mathcal{R}(\boldsymbol{\varepsilon}^s(u)) d\Omega \\ &= \frac{1}{2} \int_{\Omega} \hat{\sigma}_r^s(\mathcal{R}(\mathbf{u})) : \mathcal{R}(\boldsymbol{\varepsilon}^s) \\ &\quad + \mathcal{Q}_r(\nabla \cdot \mathcal{R}(\xi \mathbf{u} + \mathbf{U})) \nabla \cdot \mathcal{R}(\mathbf{u}) d\Omega \end{aligned}$$

is defined as the strain energy of the solid phase. The strain energy of the fluid phase reads:

$$\begin{aligned} W_{\text{def}}^f &= \frac{1}{2} \int_{\Omega} \mathcal{R}(\boldsymbol{\sigma}^f(\mathbf{u}, \mathbf{U})) : \mathcal{R}(\boldsymbol{\varepsilon}^f(u)) d\Omega \\ &= \frac{1}{2} \int_{\Omega} R_r (\nabla \cdot \mathcal{R}(\xi \mathbf{u} + \mathbf{U})) \nabla \cdot \mathcal{R}(\mathbf{U}) d\Omega. \end{aligned}$$

Concerning the dissipated powers, there is no need to separate them into solid and fluid phases.

### D. Time-averaged expressions

All the expressions given in the following are instantaneous values. As harmonic excitations are considered, it is more common to present time-averaged values. Table I summarizes the time-averaged expressions of kinetic and strain energies together with energies dissipated over a cycle through the considered mechanism. This energy is defined by  $\mathcal{W}$  with the index corresponding to the considered mechanism.  $\langle \cdot \rangle$  is the time-average operator. For this formulation it is straightforward to check that these time-averaged expressions of the stored energies and dissipated powers are the ones that can be obtained with the help of the real and imaginary part of the variational formulations.

## IV. EXPRESSIONS OF ENERGIES AND POWERS IN THE CASE OF $\{\mathbf{u}, P\}$ FORMULATION

In order to transpose the previous results obtained in the case of  $\{\mathbf{u}, \mathbf{U}\}$  formulation to the  $\{\mathbf{u}, P\}$  formulation,<sup>4</sup> a change of variable is performed. It is based on a combination of both the constitutive relation and the equation of motion of the fluid phase. Hence:

TABLE I. Summary of the energy expressions in the case of  $\{\mathbf{u}, \mathbf{U}\}$  formulation.

$\langle K_s \rangle$	$\frac{\omega^2}{4} \int_{\Omega} \rho_1  \mathbf{u}_0 ^2 d\Omega$
$\langle K_f \rangle$	$\frac{\omega^2}{4} \int_{\Omega} \rho_2  \mathbf{U}_0 ^2 - \rho'_{12}  \mathbf{u}_0 - \mathbf{U}_0 ^2 d\Omega$
$\langle W_{\text{def}} \rangle$	$\frac{1}{4} \int_{\Omega} \hat{\sigma}_r^s(\mathbf{u}_0) : \varepsilon^s(\mathbf{u}_0^*) + R_r  \xi \nabla \cdot \mathbf{u}_0 + \nabla \cdot \mathbf{U}_0 ^2 d\Omega$
$\langle \hat{W}_{\text{def}}^s \rangle$	$\frac{1}{4} \int_{\Omega} \hat{\sigma}_r^s(\mathbf{u}_0) : \varepsilon(\mathbf{u}_0^*) d\Omega$
$\langle \hat{W}_{\text{def}}^f \rangle$	$\frac{R_r}{4} \int_{\Omega}  \xi \nabla \cdot \mathbf{u}_0 + \nabla \cdot \mathbf{U}_0 ^2 d\Omega$
$\langle W_{\text{def}}^s \rangle$	$\frac{1}{4} \int_{\Omega} \hat{\sigma}_r^s(\mathbf{u}_0) : \varepsilon(\mathbf{u}_0^*) + Q_r \xi  \nabla \cdot \mathbf{u}_0 ^2 + Q_r \mathcal{R}(\nabla \cdot \mathbf{U}_0 \nabla \cdot \mathbf{u}_0^*) d\Omega$
$\langle W_{\text{def}}^f \rangle$	$\frac{R_r}{4} \int_{\Omega} \xi \mathcal{R}(\nabla \cdot \mathbf{u}_0 \nabla \cdot \mathbf{U}_0^*) +  \nabla \cdot \mathbf{U}_0 ^2 d\Omega$
$\mathcal{W}_{\text{vis}}$	$b_r \pi \omega \int_{\Omega}  \mathbf{u}_0 - \mathbf{U}_0 ^2 dS$
$\mathcal{W}_{\text{struct}}$	$\pi \int_{\Omega} \hat{\sigma}_r^s(\mathbf{u}_0) : \varepsilon(\mathbf{u}_0^*) d\Omega$
$\mathcal{W}_{\text{th}}$	$R_r \pi \int_{\Omega} \xi  \nabla \cdot \mathbf{u}_0 + \nabla \cdot \mathbf{U}_0 ^2 d\Omega$

$$\mathbf{U} = \frac{\phi}{\tilde{\rho}_{22}\omega^2} \nabla P - \frac{\tilde{\rho}_{12}}{\tilde{\rho}_{22}} \mathbf{u} \Leftrightarrow \mathbf{U}_0 = \frac{\phi}{\tilde{\rho}_{22}\omega^2} \nabla P_0 - \frac{\tilde{\rho}_{12}}{\tilde{\rho}_{22}} \mathbf{u}_0. \quad (24)$$

Recall that the apparent Biot densities are defined by

$$\tilde{\rho}_{11} = \rho_1 - \tilde{\rho}_{12}; \quad \tilde{\rho}_{22} = \rho_2 - \tilde{\rho}_{12}. \quad (25)$$

In order to obtain the expressions of the strain energies and thermal and structural dissipated powers, it is necessary to calculate  $\nabla \cdot \mathbf{U}_0$ . It is directly given by the constitutive relation of the fluid phase:

$$\nabla \cdot \mathbf{U} = -\frac{\phi}{\tilde{R}} P - \xi \nabla \cdot \mathbf{u} \Leftrightarrow \nabla \cdot \mathbf{U}_0 = -\frac{\phi}{\tilde{R}} P_0 - \xi \nabla \cdot \mathbf{u}_0. \quad (26)$$

### A. Kinetic energies and viscous dissipated power

It is possible to obtain directly both kinetic energies and viscous dissipated energies by considering the following complex quantity  $X = (4/\omega^2)\langle K^s \rangle + (4/\omega^2)\langle K^f \rangle - j(1/\pi\omega^2)\mathcal{W}_{\text{vis}}$ . Hence,  $X$  can be written as a function of the displacement amplitude:

$$X = \int_{\Omega} (\tilde{\rho}_{11} |\mathbf{u}_0|^2 + \tilde{\rho}_{12} \mathbf{u}_0^* \mathbf{U}_0 + \tilde{\rho}_{12} \mathbf{U}_0^* \mathbf{u}_0 + \tilde{\rho}_{22} |\mathbf{U}_0|^2) d\Omega. \quad (27)$$

By using Eq. (24), one obtains

$$X = \int_{\Omega} \tilde{\rho} |\mathbf{u}_0|^2 + \frac{\phi^2}{\tilde{\rho}_{22}^* \omega^4} |\nabla P_0|^2 + \frac{2j\phi}{\omega^2} \mathcal{I}\left(\frac{\tilde{\rho}_{12}}{\tilde{\rho}_{22}}\right) \mathbf{u}_0^* \nabla P_0 d\Omega. \quad (28)$$

$\tilde{\rho}$  has been introduced by Atalla *et al.*<sup>4</sup> and is defined by

$$\tilde{\rho} = \tilde{\rho}_{11} - \frac{\tilde{\rho}_{12}^2}{\tilde{\rho}_{22}}. \quad (29)$$

In order to use the modified  $\{\mathbf{u}, P\}$  formulation<sup>5</sup> it is necessary to recall the definition of the dynamic tortuosity<sup>2</sup>  $\tilde{\alpha}$  and its consequence:

$$\tilde{\alpha} = \frac{\tilde{\rho}_{22}}{\rho_2} \Rightarrow \mathcal{I}\left(\frac{\tilde{\rho}_{12}}{\rho_{22}}\right) = \mathcal{I}\left(\frac{1}{\tilde{\alpha}}\right). \quad (30)$$

Hence,

$$X = \omega^2 \int_{\Omega} \tilde{\rho} |\mathbf{u}_0|^2 + \frac{\phi^2}{\rho_{22}^* \omega^4} |\nabla P_0|^2 + \frac{2j}{\omega^2} \mathcal{I}\left(\frac{\phi}{\tilde{\alpha}}\right) \mathbf{u}_0^* \nabla P_0 d\Omega \quad (31)$$

$$\frac{\phi}{\tilde{\alpha}} = \tilde{\gamma} + h \left(1 + \frac{\tilde{Q}}{\tilde{R}}\right) \Rightarrow \mathcal{I}\left(\frac{\phi}{\tilde{\alpha}}\right) = \mathcal{I}(\tilde{\gamma}). \quad (32)$$

By identifying real and imaginary parts of  $X$ , it is possible to separate kinetic energies and viscous dissipated powers:

$$\begin{aligned} \langle K \rangle &= \frac{\omega^2}{4} \int_{\Omega} \mathcal{R}(\tilde{\rho}) |\mathbf{u}_0|^2 + \mathcal{R}\left(\frac{\phi^2}{\rho_{22}^* \omega^4}\right) |\nabla P_0|^2 \\ &\quad - \frac{2}{\omega^2} \mathcal{I}\left(\frac{\phi}{\tilde{\alpha}}\right) \mathcal{I}(\mathbf{u}_0^* \nabla P_0) d\Omega. \end{aligned} \quad (33)$$

The last expression can be separated into solid and fluid parts,

$$\langle K_s \rangle = \frac{\omega^2}{4} \int_{\Omega} \rho_1 |\mathbf{u}_0|^2 d\Omega, \quad (34)$$

$$\begin{aligned} \langle K_f \rangle &= \frac{\omega^2}{4} \int_{\Omega} \mathcal{R}(\tilde{\rho} - \rho_1) |\mathbf{u}_0|^2 + \mathcal{R}\left(\frac{\phi^2}{\rho_{22}^* \omega^4}\right) |\nabla P_0|^2 \\ &\quad - \frac{2}{\omega^2} \mathcal{I}\left(\frac{\phi}{\tilde{\alpha}}\right) \mathcal{I}(\mathbf{u}_0^* \nabla P_0) d\Omega. \end{aligned} \quad (35)$$

It is possible to define  $\tilde{\rho}_f = \tilde{\rho} - \rho_1$  in order to condense the former expression.

The imaginary part of  $X$  allows for the obtention of the viscous dissipated energy:

$$\begin{aligned} \mathcal{W}_{\text{vis}} &= -\pi\omega^2 \int_{\Omega} \mathcal{I}(\tilde{\rho}) |\mathbf{u}_0|^2 - \mathcal{I}\left(\frac{\phi^2}{\rho_{22}^* \omega^4}\right) |\nabla P_0|^2 \\ &\quad + \frac{2}{\omega^2} \mathcal{I}\left(\frac{\phi}{\tilde{\alpha}}\right) \mathcal{R}(\mathbf{u}_0^* \nabla P_0) d\Omega. \end{aligned} \quad (36)$$

This last expression agree with the ones given by Sgard *et al.*<sup>8</sup>

### B. Strain energy and thermal dissipation

Let us now consider the expressions of strain energies together with thermal and structural dissipated powers. First,

$\langle \hat{W}_{\text{def}}^s \rangle$  and  $\mathcal{W}_{\text{struct}}$  remain unchanged as they depend only on the solid displacement. A second set of expressions can easily be expressed by using Eq. (26),

$$\langle W_{\text{def}} \rangle = \frac{1}{4} \int_{\Omega} \hat{\sigma}_r^s(\mathbf{u}_0) : \boldsymbol{\varepsilon}^s(\mathbf{u}_0^*) + \frac{\phi^2 R_r}{|\tilde{R}|^2} |P_0|^2 d\Omega, \quad (37a)$$

$$\langle \hat{W}_{\text{def}}^f \rangle = \frac{\phi^2 R_r}{4|\tilde{R}|^2} \int_{\Omega} |P_0|^2 d\Omega, \quad (37b)$$

$$\mathcal{W}_{\text{th}} = \frac{\phi^2 \pi R_i}{|\tilde{R}|^2} \int_{\Omega} |P_0|^2 d\Omega. \quad (37c)$$

In order to obtain Eqs. (37b) and (37c), two intermediate results are given:

$$\begin{aligned} \int_{\Omega} |\nabla \cdot \mathbf{U}_0|^2 d\Omega &= \int_{\Omega} \left( \frac{-\phi}{\tilde{R}^*} P_0^* - \xi \nabla \cdot \mathbf{u}_0^* \right) \\ &\quad \times \left( \frac{-\phi}{\tilde{R}} P_0 - \xi \nabla \cdot \mathbf{u}_0 \right) d\Omega \\ &= \int_{\Omega} \frac{\phi^2}{|\tilde{R}|^2} |P_0|^2 + 2\phi\xi\mathcal{R} \left( \frac{\nabla \cdot \mathbf{u}_0^* P_0}{\tilde{R}} \right) \\ &\quad + \xi^2 |\nabla \cdot \mathbf{u}_0|^2 d\Omega, \end{aligned}$$

$$\begin{aligned} \int_{\Omega} \mathcal{R}(\nabla \cdot \mathbf{u}_0 \nabla \cdot \mathbf{U}_0^*) d\Omega &= - \int_{\Omega} \mathcal{R} \left( \frac{\phi}{\tilde{R}^*} \nabla \cdot \mathbf{u}_0 P_0^* \right) \\ &\quad + \xi |\nabla \cdot \mathbf{u}_0|^2 d\Omega. \end{aligned}$$

Therefore,

$$\langle W_{\text{def}}^s \rangle = \frac{1}{4} \int_{\Omega} \hat{\sigma}_r^s(\mathbf{u}_0) : \boldsymbol{\varepsilon}(\mathbf{u}_0^*) - Q_r \mathcal{R} \left( \frac{\phi^2}{\tilde{R}^*} \nabla \cdot \mathbf{u}_0 P_0^* \right) d\Omega, \quad (38)$$

$$\langle W_{\text{def}}^f \rangle = \frac{R_r}{4} \int_{\Omega} \xi \phi \mathcal{R} \left( \frac{\nabla \cdot \mathbf{u}_0 \cdot P_0^*}{\tilde{R}^*} \right) + \frac{\phi^2}{|\tilde{R}|^2} |P_0|^2 d\Omega. \quad (39)$$

All the results for the modified  $\{\mathbf{u}, P\}$  formulation are summarized in Table II.

### C. Discussion

It is necessary to underline that the  $\{\mathbf{u}, P\}$  expressions of the stored energies proposed in Sec. IV B are not the ones which can be obtained by taking the real part of the classically called mixed poroelastic variational formulations.<sup>4</sup> This identification, well known as a classical vibration problem [as well as the  $\{\mathbf{u}, \mathbf{U}\}$  formulation], is not valid in this case. The reason for this difference lies in the derivation of the mixed formulation,<sup>4</sup> which is not obtained from the differentiation of a Lagrangian density dealing with the whole porous material (solid and fluid phase). The methodology is in fact in two steps; the first one is the obtention of motion equations in terms of  $\{\mathbf{u}, P\}$  fields for each phase. The second step of the method of Attala *et al.* is to multiply by an ad-

TABLE II. Summary of the energy expressions in the case of modified  $\{\mathbf{u}, P\}$  formulation.

$\langle K_s \rangle$	$\frac{\omega^2}{4} \int_{\Omega} \rho_1  \mathbf{u}_0 ^2 d\Omega$
$\langle K_f \rangle$	$\frac{\omega^2}{4} \int_{\Omega} \mathcal{R}(\tilde{\rho}_j)  \mathbf{u}_0 ^2 + \mathcal{R} \left( \frac{\phi^2}{\rho_{22}^* \omega^4} \right)  \nabla P_0 ^2$ $- \frac{2}{\omega^2} \mathcal{I} \left( \frac{\phi}{\tilde{\alpha}} \right) \mathcal{I}(\mathbf{u}_0^* \nabla P_0) d\Omega$
$\langle W_{\text{def}} \rangle$	$\frac{1}{4} \int_{\Omega} \hat{\sigma}_r^s(\mathbf{u}_0) : \boldsymbol{\varepsilon}^s(\mathbf{u}_0^*) + \frac{\phi^2 R_r}{ \tilde{R} ^2}  P_0 ^2 d\Omega$
$\langle \hat{W}_{\text{def}}^s \rangle$	$\frac{1}{4} \int_{\Omega} \hat{\sigma}_r^s(\mathbf{u}_0) : \boldsymbol{\varepsilon}(\mathbf{u}_0^*) d\Omega$
$\langle \hat{W}_{\text{def}}^f \rangle$	$\frac{\phi R_r}{4 \tilde{R} ^2} \int_{\Omega}  P_0 ^2 d\Omega$
$\langle W_{\text{def}}^s \rangle$	$\frac{1}{4} \int_{\Omega} \hat{\sigma}_r^s(\mathbf{u}_0) : \boldsymbol{\varepsilon}(\mathbf{u}_0^*) - Q_r \mathcal{R} \left( \frac{\phi}{\tilde{R}^*} \nabla \cdot \mathbf{u}_0 P_0^* \right) d\Omega$
$\langle W_{\text{def}}^f \rangle$	$\frac{R_r}{4} \int_{\Omega} \xi \phi \mathcal{R} \left( \frac{\nabla \cdot \mathbf{u}_0 \cdot P_0^*}{\tilde{R}^*} \right) + \frac{\phi^2}{ \tilde{R} ^2}  P_0 ^2 d\Omega$
$\mathcal{W}_{\text{vis}}$	$-\pi \omega^2 \int_{\Omega} \mathcal{I}(\tilde{\rho})  \mathbf{u}_0 ^2 - \mathcal{I} \left( \frac{\phi^2}{\rho_{22} \omega^4} \right)  \nabla P_0 ^2$ $+ \frac{2}{\omega^2} \mathcal{I} \left( \frac{\phi}{\tilde{\alpha}} \right) \mathcal{R}(\mathbf{u}_0^* \nabla P_0) d\Omega$
$\mathcal{W}_{\text{struct}}$	$\pi \int_{\Omega} \hat{\sigma}_i^s(\mathbf{u}_0) : \boldsymbol{\varepsilon}(\mathbf{u}_0^*) d\Omega$
$\mathcal{W}_{\text{th}}$	$\frac{\phi^2 \pi R_i}{ \tilde{R} ^2} \int_{\Omega}  P_0 ^2 d\Omega$

missible field each one of these two motion equations. Hence, two bilinear formulations are then obtained. The global mixed formulation is obtained by adding equations of the solid and fluid phase. It is interesting to note that every combination of these two equations could have been used. Several differences occur while comparing this sum to the expressions given in Sec. IV B.<sup>4,5,8</sup>

Despite the remarks of this section, it is fundamental to indicate that the numerical results obtained through the finite-element discretization of the mixed formulations based on Ref. 4 are correct even if the energetic interpretation of these formulations must be handled with care. This is confirmed in Sec. V.

## V. APPLICATION TO A MULTILAYERED PROBLEM

### A. Presentation of the problem

The following is devoted to the adaptation of the analytical energetic indicators proposed in the preceding sections to a discretized problem. The convergence of finite element schemes is often made through global indicators, it is then interesting to use the proposed ones. They are complementary to the mathematical  $\mathcal{L}^2$  ones (mean square pressure or velocity, for example) which do not have physical significance. It is then necessary to investigate in which way they are able to check the validity of a finite-element discretization.

The configuration of interest is a monodimensional two layer problem depicted in Fig. 1. The second layer is bonded on a rigid wall and the first one is excited by a normalized pressure plane wave. The properties of the two porous media are given in Table III and the Appendix presents the expres-

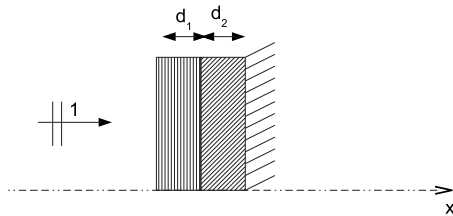


FIG. 1. Configuration of the problem.

sions of the coefficients of the Biot–Allard<sup>2</sup> model. This problem is numerically interesting as the acoustical behavior of these two porous materials is more complex than the case for a single porous structure. The second advantage is that an exact analytical solution can be obtained. Hence, the accuracy of the discretization scheme can be estimated by a comparison to the exact analytical solution of the problem considered as reference. It is not the case of the convergence analysis of poroelastic finite element models of the literature for which the reference solution is a numerical overmeshed discretized result.

## B. Physical considerations

This simple problem can be solved analytically and the methodology is as follows. The shear waves are not excited by the normal incident plane wave and only the two compressional waves are involved. The solid and fluid displacements and the pressure can be written as a function of the amplitude of these waves (similar to Allard’s<sup>2</sup> methodology). Nine unknowns are then involved (eight amplitude unknowns and the reflection coefficient  $R$  at the air–porous interface). The problem can be solved by way of the nine following relations. At the rigid backing interface, one has two relations: cancellation of the solid and total displacement<sup>13</sup> [defined by  $\mathbf{u}' = (1 - \phi)\mathbf{u} + \phi\mathbf{U}$ ]. At the two porous substructure interface, four continuity relations are involved (solid and total displacement, *in vacuo* stress tensor<sup>13</sup> and pressure). At the air–porous interface there are three relations: the air displacement is equal to the porous structure total displacement, the *in vacuo* stress is null, and the pressure is continuous. It is then possible to solve analytically this nine linear equation system with Cramer’s determinant, to find the amplitudes of the eight waves and then to deduce the analytical expressions of the solid displacement and the

TABLE III. Material properties.

		Material 1	Material 2
$\phi$	(1)	0.952	0.937
$\sigma$	(Ns m <sup>-4</sup> )	21300	50485
$\alpha_\infty$	(1)	1.9	2.57
$\Lambda$	( $\mu\text{m}$ )	100	57.41
$\Lambda'$	( $\mu\text{m}$ )	300	61.62
$\rho_1$	(kg m <sup>-3</sup> )	38.4	95.66
$E$	(kPa)	30	66
$\eta_s$	(1)	0.04	0.105
$d$	(cm)	5	5

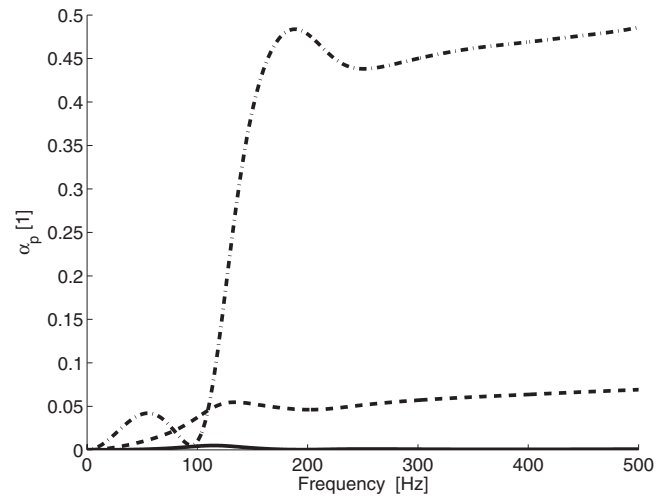


FIG. 2. Partial absorption coefficient of the first layer. Solid line: Structural dissipation; dashed line: Thermal effects; and dash-dot line: Viscous effects.

pressure. The energetic indicator of Tables I and II can be deduced through a formal spatial integration.

It is interesting to first analyze the physics of the problem in order to point out the interest of energetic indicators. All the results presented in this section correspond to the analytical ones. Figures 2 and 3, respectively, present the partial absorption of the left and the right layer in the [1;500] Hz frequency band. (1) means nondimensional parameter. The classical absorption coefficient is defined as the ratio of the absorbed power over the incident one. Each one of these six partial absorption coefficients involves the restriction of this ratio to a particular mechanism for a considered layer. For example, the dash-dotted curve of Fig. 2 represents the dissipation by viscous effects in the first layer:

$$\alpha_{\text{vis}}^l = \frac{W_{\text{vis}}^l}{W_{\text{vis}}^l + W_{\text{struct}}^l + W_{\text{th}}^l + W_{\text{vis}}^r + W_{\text{struct}}^r + W_{\text{th}}^r} (1 - |R|^2). \quad (40)$$

The  $l$  and  $r$  exponents are related to the left and right layer, respectively. These figures clearly show that viscous effects

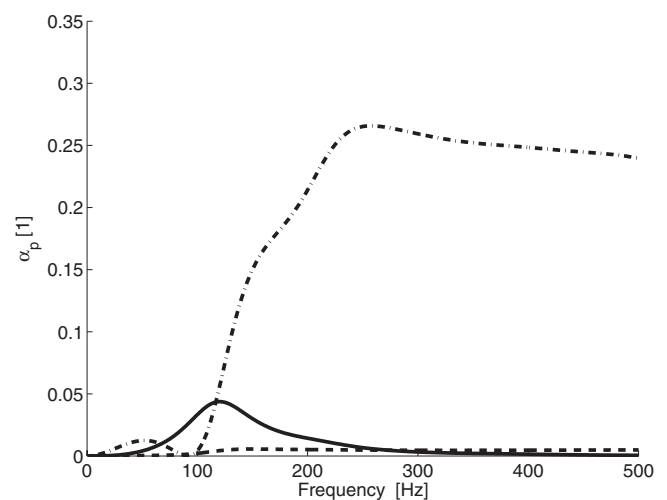


FIG. 3. Partial absorption coefficient of the second layer. Solid line: Structural dissipation; dashed line: Thermal effects; and dash-dot line: Viscous effects.

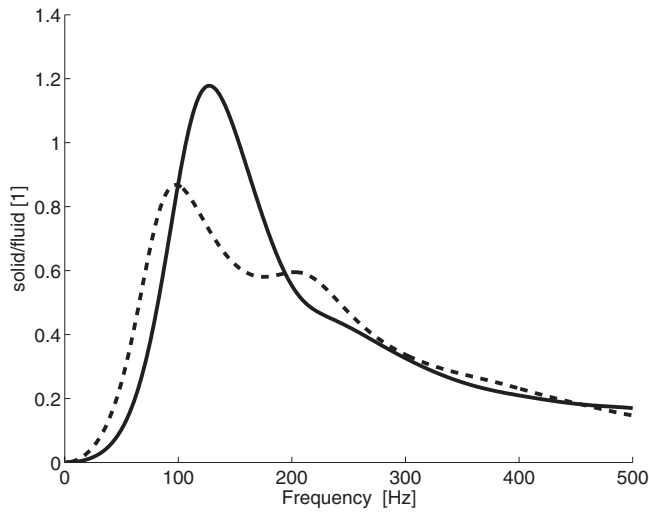


FIG. 4. Ratio of the mean total energy in the solid phase over the fluid one. Solid line: first layer and dashed line: Second layer.

correspond to the major dissipation mechanism. It is a general comment which is well known for sound-absorbing materials. In particular, it is interesting to notice that, at the resonance frequency of the solid wave (around 90 Hz), the viscous effects vanish thereby reducing the global absorption of the system. In addition, the resonance of the fluid wave (around 200 Hz) corresponds to a maximum of absorption of the material induced by a strong contribution of viscous effects. In addition, the relative influence of thermal and structural effects mainly depends on the properties of the materials: In the left layer, structural effects are predominant and in the right layer, thermal effects are predominant. This difference is of course explained by the comparison of structural coefficients  $\eta_s$  and acoustical parameters of both materials.

Figure 4 presents the ratio of the mean total energy in the solid phase over the one of the fluid phase. It is of interest to obtain the resonance of the solid-borne waves corresponding to a maximum of this function. The maximum in the first and second layers do not perfectly coincide as the properties of the Biot waves are different, but they are close due to the boundary conditions between the structures inducing a strong coupling of the solid phases of both materials. It can also be noticed that for higher frequencies, the energy is mainly in the fluid phase as suggested by Zwikker and Kosten<sup>14</sup> and Biot.<sup>1,2</sup>

Figure 5 presents both the ratio of total mean energy and dissipated power of the first layer over the second one. Energy is of course mainly in the first layer than in the second one. It can be easily explained by pointing out that the acoustical wave enters by the left layer and that the second structure is bonded then vanishing the solid and fluid displacements at the end of the material. A noticeable difference between the conservative curve and the dissipative one can be observed. There is no physical reason for an agreement of these indicators and it can be checked that the one corresponding to dissipated powers is most influenced by the resonance of the solid and fluid waves.

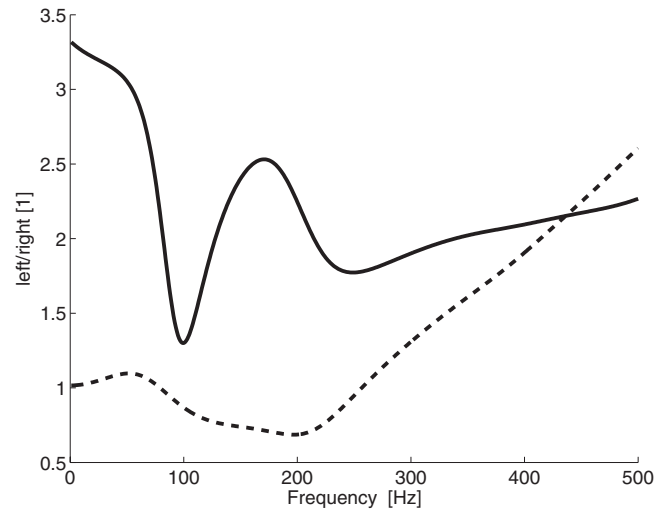


FIG. 5. Ratio of the left layer over the right one. Solid line: Total dissipated power and dashed line: Mean total energy.

### C. Convergence analysis

Several convergence studies of poroelastic finite-element schemes were published in the past.<sup>15–17</sup> The methods proposed in these works could be considered as qualitative in the sense that the convergence was shown and analyzed but not compared to a model. In this paper, an alternative method is proposed on a simple multilayer case. The main objective of this section is to study the convergence of the finite element method with the energetic indicators and to obtain quantitative estimation of the validity of the discretization by a comparison to a theoretical convergence model. A finite-element scheme is of order  $d$  if

$$\|X - X_h\|_I \approx C(I, \omega)h^d, \quad (41)$$

where  $X$  and  $X_h$  are the exact and discretized solution,  $\|\cdot\|_I$  is the norm associated with indicator  $I$ .  $h$  is the spatial discretization step.  $C(I, \omega)$  is a quantitative parameter of the convergence and  $d$  corresponds to the order of the interpolation set. Relation (41) is more tractable in logarithm representation:

$$\log(\|X - X_h\|_I) \approx \log[C(I, \omega)] + d \log(h). \quad (42)$$

Hence the logarithm of the relative error is an affine function of the logarithm of the discretization step whose slope (respectively, y intercept) is  $d$  (respectively,  $\log[C(I, \omega)]$ ). The problem is discretized with both  $\{\mathbf{u}, \mathbf{U}\}$  and  $\{\mathbf{u}, P\}$  linear elements with a regular spatial mesh. The numerical simulations have been done in a frequency range from 100 to 3500 Hz with a 25 Hz step. For each frequency the substructures are meshed with the same number of nodes. This number of nodes goes from 5 to 300. Hence, more than 80 000 numerical simulations ( $137 \times 296 \times 2$ ) were performed. Three-hundred nodes for each layer are of course not necessary to obtain an adequate solution in terms of industrial classical approximation. It is nevertheless interesting from a numerical point of view as it confirms for very refined meshes the results obtained for standard ones.<sup>18</sup>

Figure 6 (respectively, Fig. 7) presents the convergence of the mean total energy (respectively, mean total dissipated



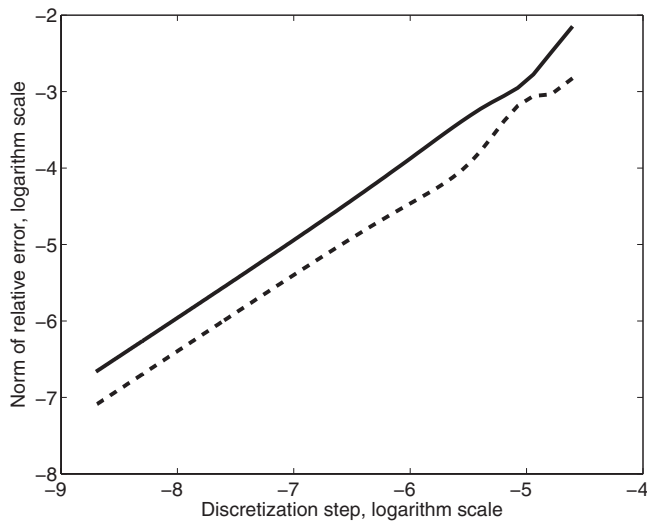


FIG. 6. Convergence of the mean total stored energy. Solid line:  $\{\mathbf{u}, \mathbf{U}\}$  formulation and dashed line:  $\{\mathbf{u}, P\}$  formulation.

energy) of the whole structure at 1 kHz in a log–log representation. The error is plotted as a function of the discretization step. In the considered case, both material layers have the same discretization step to simplify the graphical representation, nevertheless additional numerical investigation not shown here for sake of conciseness allows one to generalize these results even when the discretization steps of the two layers are different.

It can be noticed that both relative errors tend to zero with the discretization step. This means that both  $\{\mathbf{u}, \mathbf{U}\}$  and  $\{\mathbf{u}, P\}$  discretization converge toward the exact analytical value. Hence, even if there is an energetic ambiguity with the mixed formulation, the authors want to underline once more that there is no doubt about the results of the finite-element discretization. In addition, it is also interesting to add a comment on the order of the convergence. The two proposed results (Figs. 6 and 7) are representative of the whole set of simulations and one can identify an affine function of slope around 1. This result means that the order  $d$  of the conver-

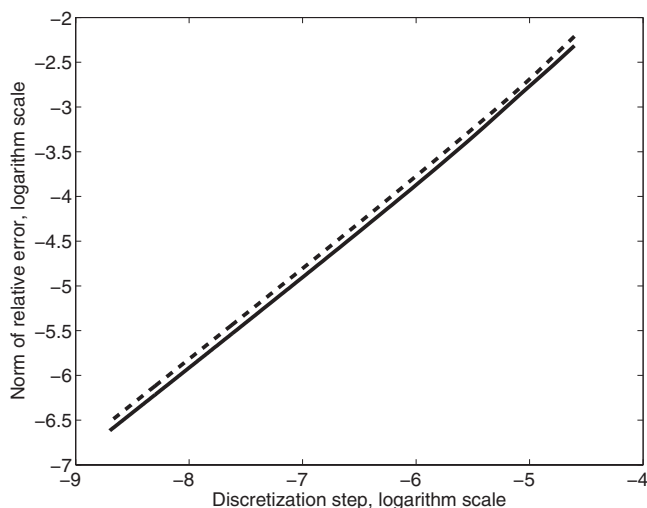


FIG. 7. Convergence of the mean total dissipated power. Solid line:  $\{\mathbf{u}, \mathbf{U}\}$  formulation and dashed line:  $\{\mathbf{u}, P\}$  formulation.

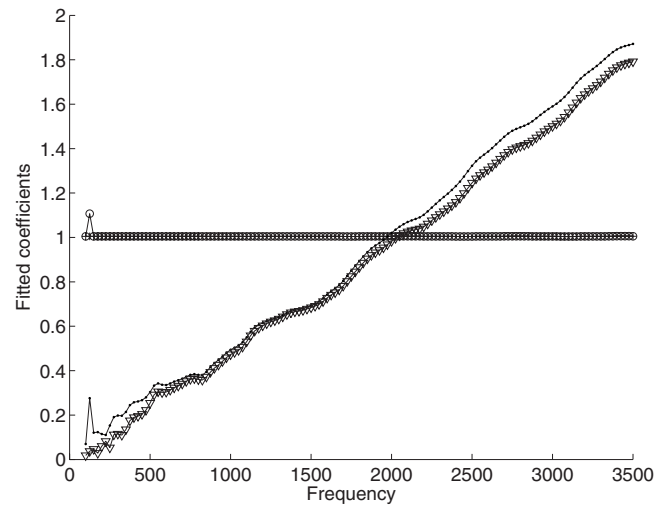


FIG. 8. Evolution of the fitted coefficients for  $K_f$ , second substructure. (○)  $\{\mathbf{u}, \mathbf{U}\}$  formulation  $d$ ; (+)  $\{\mathbf{u}, P\}$  formulation  $d$ ; (⋯)  $\{\mathbf{u}, \mathbf{U}\}$  formulation  $\log(C(I, \omega))/60$ ; (▽)  $\{\mathbf{u}, P\}$  formulation  $\log(C(I, \omega))/60$ .

gence of linear finite element for these two energetic indicators is equal to unity. Figures 6 and 7 enable one to identify the value of the convergence parameters  $C(I, \omega)$  as the exponential of the  $y$  intercept of the linear interpolation line. This value is a function of  $\omega$  as the physical parameters of the model are themselves functions of the pulsation.

A fitting process has been done on the whole set of simulations. It is as follows: For each frequency, relations (42) are fitted and  $d$  and  $C(I, \omega)$  are obtained. Figure 8 shows the evolution of these two parameters  $C(I, \omega)$  and  $d$  versus the frequency for the kinetic energy of the fluid phase of the second substructure. The value of  $C(I, \omega)$  is divided by 60 in order to plot the two evolutions on the same graph. It can be noticed that for both formulations the order  $d$  is really close to one for each frequency thereby validating that the energetic convergence of the finite-element scheme for linear poroelastic elements is unity. This has been observed for all the other indicators. In addition, function  $C(I, \omega)$  is always a crossing function of  $\omega$ . The spatial step must be shortened with increasing frequencies. It can also be noticed that the frequency evolution of  $C(I, \omega)$  can be fitted through a linear interpolation in this case. It is unfortunately not possible to obtain a general interpolation for  $C(I, \omega)$  law available for all indicators.

This numerical study proposed a methodology to obtain the quantitative parameters of the convergence of linear finite elements for the proposed indicators. This result shows that the proposed energetic indicators may be used to evaluate the convergence of finite element schemes and that the order of convergence is equal to one for all of them. Even if this result could seem natural, it has never been checked. Further investigations must be undertaken in order to model the evolution of  $C(I, \omega)$  and it is a perspective of this paper.

## VI. CONCLUSION

This paper was devoted to the rigorous obtention of stored energies (kinetic and strain) and dissipated ones for porous materials described by the Biot–Allard model ex-

pressed in  $\{\mathbf{u}, \mathbf{U}\}$  and  $\{\mathbf{u}, P\}$  formulations. It has been shown that the classical techniques dealing with the real and imaginary parts of the variational formulations are not valid and must be handled with care. The methodology was based on the mechanics and thermodynamics of open porous continua.<sup>11</sup> Both kinetic and strain mean energies have been given and separated into solid and fluid parts. The expressions of energies dissipated over a cycle were also provided for the three dissipation mechanisms. These expressions could be very useful to identify the contributions of the different dissipation mechanisms to the sound absorption or the damping induced by a sound package.

A numerical example has been considered to illustrate the theoretical results. First, the validity of the analytical expressions given in the preceding sections has been demonstrated. Second, the convergence of the finite element method has been shown to be of order one for the considered energetic indicators. A methodology to obtain the quantitative parameters of the convergence has also been applied to a simplified case and must be furthered. It seems then interesting to use these indicators to evaluate the convergence of finite element methods.

#### APPENDIX: TOPICS ON BIOT–ALLARD MODEL

This Appendix provides the expressions of the inertial and constitutive parameters of the Biot–Allard model. All these expressions can be found in Allard.<sup>2</sup> This model allows one to find the expressions of the coefficient used in the manuscript as a function of the material properties of Table III. These expressions are given for a circular frequency  $\omega$ .

The viscous effects are modeled through  $\tilde{b}$  coefficient whose expression is

$$\tilde{b} = j\omega\phi\rho_0(\tilde{\alpha} - \alpha_\infty), \quad (\text{A1})$$

where  $\alpha_\infty$  is the geometric tortuosity,  $\phi$  is the porosity, and  $\rho_0$  is the density of the air.  $\tilde{\alpha}$  is the dynamic tortuosity defined by

$$\tilde{\alpha} = 1 - \frac{j\phi\sigma}{\alpha_\infty\rho_0\omega} \sqrt{1 - \frac{4j\alpha_\infty^2\eta_a\rho_0\omega}{(\sigma\Lambda\phi)^2}}, \quad (\text{A2})$$

$\sigma$  is the flow resistivity,  $\eta_a$  is the dynamic viscosity of air, and  $\Lambda$  is the viscous characteristic length. The thermal properties are given by the dynamic compressibility  $\tilde{K}_{\text{eq}}$ :

$$\tilde{K}_{\text{eq}} = \frac{\gamma P_0}{\gamma - (\gamma - 1) \left[ 1 + \frac{8\eta_a}{j\Lambda' \text{Pr}\omega\rho_0} \sqrt{1 + \frac{j\rho_0\omega \text{Pr}\Lambda'^2}{16\eta_a}} \right]}, \quad (\text{A3})$$

where  $\Lambda'$  is the thermal characteristic length, Pr is the Prandtl number,  $P_0$  is the ambient pressure, and  $\gamma$  is the ratio of specific heats of air. For sound-absorbing materials, one has

$$\tilde{Q} = \phi(1 - \phi)\tilde{K}_{\text{eq}}, \quad \tilde{R} = \phi^2\tilde{K}_{\text{eq}}. \quad (\text{A4})$$

The structural mechanical parameters  $N$  and  $\hat{A}$  are given by

$$N = \frac{E(1 + j\eta_s)}{2(1 + \nu)}, \quad \hat{A} = \frac{2N\nu}{1 - 2\nu}. \quad (\text{A5})$$

- <sup>1</sup>M. A. Biot, "Theory of propagation of elastic waves in a fluid-saturated porous solid. I. Low frequency range," *J. Acoust. Soc. Am.* **28**, 168–178 (1956).
- <sup>2</sup>J. Allard, *Propagation of Sound in Porous Media, Modelling Sound Absorbing Materials* (Elsevier Application Science, Amsterdam, 1993).
- <sup>3</sup>B. R. Simon, J. S. S. Wu, O. C. Zienkiewicz, and D. K. Paul, "Evaluation of u-w and u- $\pi$  finite element formulation for the dynamic response of saturated porous media using one-dimensional models," *Int. J. Numer. Analyt. Meth. Geomech.* **10**, 461–482 (1986).
- <sup>4</sup>N. Atalla, R. Panneton, and P. Debergue, "A mixed displacement-pressure formulation for poroelastic materials," *J. Acoust. Soc. Am.* **104**, 1444–1452 (1998).
- <sup>5</sup>N. Atalla, M. A. Hamdi, and R. Panneton, "Enhanced weak integral formulation for the mixed {u,P} poroelastic equations," *J. Acoust. Soc. Am.* **109**, 3065–3068 (2001).
- <sup>6</sup>R. Panneton and N. Atalla, "An efficient finite element scheme for solving the three-dimensional poroelasticity problem in acoustics," *J. Acoust. Soc. Am.* **101**, 3287–3298 (1997).
- <sup>7</sup>P. Göransson, "A 3d, symmetric finite element formulation of the Biot equations with application to acoustic wave propagation through an elastic porous medium," *Int. J. Numer. Methods Eng.* **41**, 167–192 (1998).
- <sup>8</sup>F. C. Sgard, N. Atalla, and J. Nicolas, "A numerical model for the low frequency diffuse field sound transmission loss of double-wall sound barriers with elastic porous linings," *J. Acoust. Soc. Am.* **108**, 2865–2872 (2000).
- <sup>9</sup>O. Dazel, F. Sgard, C.-H. Lamarque, and N. Atalla, "An extension of complex modes for the resolution of finite-element poroelastic problems," *J. Sound Vib.* **253**, 421–445 (2001).
- <sup>10</sup>O. Dazel, F. Sgard, and C.-H. Lamarque, "Application of generalized complex modes for the calculation of the forced response of three dimensional porous structures," *J. Sound Vib.* **268**, 555–580 (2003).
- <sup>11</sup>O. Coussy, *Mechanics of Porous Continua* (Wiley, New York, 1995).
- <sup>12</sup>M. A. Biot and D. G. Willis, "The elastic coefficients of the theory of consolidation," *J. Appl. Mech.* **24**, 179–191 (1957).
- <sup>13</sup>O. Dazel, B. Brouard, C. Depollier, and S. Griffiths, "An alternative Biot's displacement formulation for porous materials," *J. Acoust. Soc. Am.* **121**, 3509–3516 (2007).
- <sup>14</sup>C. Zwikker and C. Kosten, *Sound Absorbing Materials* (Elsevier, New York, 1949).
- <sup>15</sup>N. Dauchez, S. Sahraoui, and N. Atalla, "Convergence of poroelastic finite elements based on Biot displacement formulation," *J. Acoust. Soc. Am.* **109**, 33–40 (2001).
- <sup>16</sup>N.-E. Hörlin, M. Nordström, and P. Göransson, "A 3D hierarchical FE formulation of Biot's equations for elasto-acoustic modelling of porous media," *J. Sound Vib.* **245**, 633–652 (2001).
- <sup>17</sup>S. Rigobert, N. Atalla, and F. C. Sgard, "Investigation of the convergence of the mixed displacement-pressure formulation for three-dimensional poroelastic materials using hierarchical elements," *J. Acoust. Soc. Am.* **114**, 2607–2617 (2003).
- <sup>18</sup>O. Dazel, "Component mode synthesis for porous media," Ph.D., Insa de Lyon 2003 (In French).